

Synthesis and ionic transport of sulfonated ring-opened polynorbornene based copolymers

Arlette A. Santiago^a, Joel Vargas^a, Javier Cruz-Gómez^a, Mikhail A. Tlenkopatchev^{b,*}, Rubén Gaviño^c, Mar López-González^{d,*}, Evaristo Riande^d

^aFacultad de Química, Universidad Nacional Autónoma de México, CU, Coyoacán, México DF 04510, México

^bInstituto de Investigaciones en Materiales, Universidad Nacional Autónoma de México, Apartado Postal 70-360, CU, Coyoacán, México DF 04510, México

^cInstituto de Química, Universidad Nacional Autónoma de México, CU, Coyoacán, México DF 04510, México

^dInstituto de Ciencia y Tecnología de Polímeros (CSIC), 28006 Madrid, Spain

ARTICLE INFO

Article history:

Received 16 March 2011

Received in revised form

18 July 2011

Accepted 22 July 2011

Available online 27 July 2011

Keywords:

Sulfonated polynorbornene

Ionic transport

Monomer reactivity

ABSTRACT

The *N*-pentafluorophenyl-*exo-endo*-norbornene-5,6-dicarboximide (**1a**) and *N*-phenyl-*exo-endo*-norbornene-5,6-dicarboximide (**1b**) monomers were synthesized and copolymerized via ring opening metathesis polymerization (ROMP) using bis(tricyclohexylphosphine)benzylidene ruthenium(IV) dichloride (**I**) and tricyclohexylphosphine[1,3-bis(2,4,6-trimethylphenyl)-4,5-dihydroimidazol-2-ylidene][benzylidene] ruthenium dichloride (**II**). Experiments, at distinct monomer molar ratios, were carried out using catalyst **I** in order to determine the copolymerization reactivity constants by applying the Mayo-Lewis and Fineman-Ross methods. Moreover, both catalysts were used to produce random and block high molecular weight copolymers of **1a** with **1b** and **1a** with norbornene (**NB**) which were further hydrogenated using a Wilkinson's catalyst. Then, the saturated copolymers underwent a nucleophilic aromatic substitution by reacting with sodium 4-hydroxybenzenesulfonate dihydrate to generate new polynorbornene ionomers bearing fluorinated pendant benzenesulfonate groups. A thorough study on the electrochemical characteristics involving electromotive forces of concentration cells and proton conductivity of cation-exchange membranes based on a block copolymer of norbornene dicarboximides containing structural units with phenyl and fluorinated pendant benzenesulfonate moieties is reported. The study of electromotive forces (*emf*) of concentration cells with the sulfonated membrane of copolymer **8** separating electrolyte solutions of different concentration indicate that the membranes exhibit high permselectivity to protons and sodium ions at moderately low concentrations. In principle, these results suggest that the membranes can be considered candidates for ionic separation applications.

© 2011 Elsevier Ltd. All rights reserved.

1. Introduction

Copolymerization is a valuable tool for the synthesis of novel materials because it allows tuning of the thermal, mechanical and ionic, among other polymer properties. Owing to this versatility, materials suitable for applications ranging from electronics to drug delivery can be obtained [1,2]. However, in order to determine and foretell the copolymer composition, mechanistic and kinetic understanding is of great importance and several studies have been focused on this issue in the past [3,4].

The ROMP has been used to synthesize well controlled copolymers of norbornene derivatives for gas transport applications [5,6].

Taking into account that the development of fluorine containing polymeric materials displaying outstanding properties for specialty applications is an evolving area in materials science, norbornenes bearing fluorinated substituents and subjected to ROMP using a wide variety of transition metal compounds have been studied [7–9]. The presence of fluorine containing moieties in the polynorbornene dicarboximide structures has shown to be effective to improve gas permeability due to an increase of the interactions between the gases and the polar fluorinated moieties as well as in the free volume which in turns facilitates the diffusion of the gas molecules through the polymer [10,11]. In particular, sorption studies carried out recently on membranes of polynorbornene with pentafluorophenyl moieties attached to the dicarboximide side groups showed a significant increase in gas solubility [12]. Pentafluorophenyl moieties also provide the possibility of further modifications. They are highly reactive towards the nucleophilic aromatic substitutions and multiblock copolymers have been

* Corresponding authors. Tel.: +00 52 5556224586; fax: +00 52 5556161201.
E-mail addresses: tma@servidor.unam.mx (M.A. Tlenkopatchev), mar@ictp.csic.es (M. López-González).

successfully prepared by a polycondensation reaction between fluorinated oligomers and hydroxyl-terminated telechelics under basic conditions in polar, aprotic solvents [13].

Ionomers with hydrocarbon backbones prepared by the sulfonation of polynorbornene and its derivatives are attractive as proton exchange membranes since the hydrophilic and hydrophobic domains of a polynorbornene bearing polar strong acid groups (e.g. sulfuric acid) promote phase segregation resulting in conductance from the migration of protons through channels [14,15]. In addition, ultrathin ionomer films, obtained from the sulfonation of surface-initiated polynorbornene with acetyl sulfate, have reported to exhibit low resistances against proton transport [16]. The tailorable functionality of norbornene-based monomers has encouraged the quest for polyionic materials suitable not only as polymer electrolyte membrane in fuel cells but also for the construction of light emitting devices (LED) by sequential adsorption of sulfonated polynorbornenes [17], among other applications. Based on the high reactivity of the pentafluorinated rings, a new ionomer bearing highly fluorinated pendant benzenesulfonate groups has lately been synthesized by the reaction of the hydrogenated poly(*N*-pentafluorophenyl-norbornene-5,6-dicarboximide) with sodium 4-hydroxybenzenesulfonate dihydrate [18].

In the present study, norbornene copolymers containing fluorinated dicarboxylic imide side moieties were prepared through ROMP using bis(tricyclohexylphosphine)benzylidene ruthenium(IV) dichloride (**I**) and tricyclohexylphosphine[1,3-bis(2,4,6-trimethylphenyl)-4,5-dihydroimidazol-2-ylidene][benzylidene] ruthenium dichloride (**II**).

Low conversion copolymerizations were carried out using catalyst **I**. Then, the compositions of copolymers were determined by ¹H NMR and the reactivity ratios were calculated from the initial monomer feed by applying the Mayo-Lewis [19] and Finemann-Ross [20] methods, respectively. We have reported the synthesis and ionic transport performance of a non-fluorinated ionic polynorbornene dicarboximide [14,15], therefore we have envisioned the synthesis of high molecular weight copolymers, their homogeneous post-hydrogenations and even further sulfonations to obtain copolymers bearing fluorinated pendant benzenesulfonate groups. Afterwards, we investigated the ionic permselectivity and proton conductivity of membranes prepared from a copolymer of **1a** and **1b** for evaluating its potential application as ionomer. To do so, the electromotive forces of the concentration potential cells of sulfonated copolymer **8** membranes were measured keeping the ratio between the concentrations of the concentrated and dilute compartments in the vicinity of two. As electrolytes, hydrochloric acid and sodium chloride solutions were used, respectively. From the electromotive forces the counterion transport numbers were obtained and the effect of the concentration of the electrolyte solutions on the counterion transport number was determined.

2. Experimental part

2.1. Techniques

¹H NMR, ¹³C NMR and ¹⁹F NMR spectra were recorded on a Varian spectrometer at 300, 75 and 282 MHz, respectively, in deuterated chloroform (CDCl₃), *N,N*-dimethylformamide (DMF-*d*₇) and dimethylsulfoxide (DMSO-*d*₆). Tetramethylsilane (TMS) and trifluoroacetic acid (TFA) were used as internal standards, respectively. Glass transition temperatures, *T*_g, were determined in a DSC-7 Perkin Elmer Inc., at scanning rate of 10 °C/min under nitrogen atmosphere. The samples were encapsulated in standard aluminum DSC pans. Each sample was run twice on the temperature range between 30 °C and 300 °C under nitrogen atmosphere. The *T*_g values obtained were confirmed by TMA from the first

heating cycle conducted at a rate of 10 °C/min under nitrogen atmosphere with a TA Instruments Thermomechanical Analyzer TMA 2940. Onset of decomposition temperature, *T*_d, was determined using thermogravimetric analysis, TGA, which was performed at a heating rate of 10 °C/min under nitrogen atmosphere with a DuPont 2100 instrument. FT-IR spectra were obtained on a Thermo Nicolet 6700 spectrometer. Molecular weights and molecular weight distributions were determined with reference to polystyrene standards on a Waters 2695 ALLIANCE GPC at 35 °C in tetrahydrofuran using a universal column and a flow rate of 0.5 mL min⁻¹. X-ray diffraction measurements of copolymer films as cast were carried out in a Siemens D-5000 diffractometer between 4 and 70° 2θ, at 35 KV 25 mA, using CuK_α radiation (1.54 Å). Mechanical properties under tension, Young's modulus (*E*) and stress (*σ*), were measured in a Universal Mechanical Testing Machine Instron 1125-5500R using a 50 Kg cell at a crosshead speed of 10 mm/min according to the method ASTM D1708 in film samples of 0.5 mm of thickness at room temperature. Tapping mode atomic force microscopy (TM-AFM) was performed in air using a Scanning Probe Microscope Jeol JSPM-4210 with a NSC12 μmasch needle (an ultra-sharp silicon probe cantilever provided by the company MikroMasch, San Jose, CA, USA). The samples were imaged at ambient conditions.

2.2. Reagents

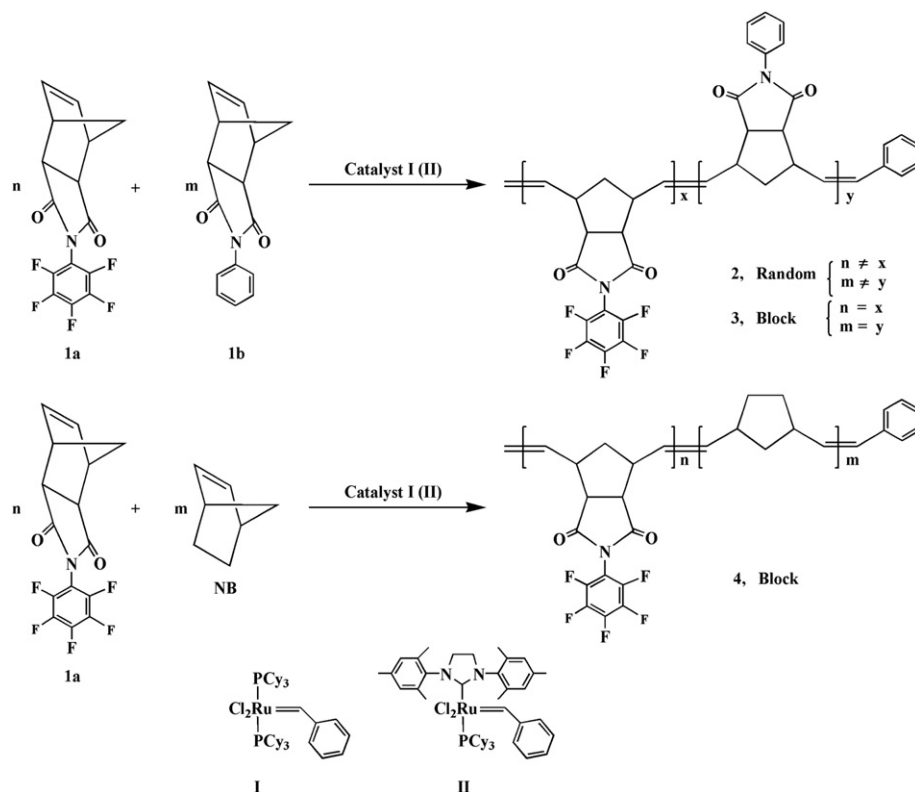
Norbornene-5,6-dicarboxylic anhydride (**NDA**) was prepared via Diels–Alder condensation of cyclopentadiene and maleic anhydride according to literature [14]. *Exo*(75%)–*endo*(25%) monomer mixture of *N*-pentafluorophenyl-norbornene-5,6-dicarboximide (**1a**) and *exo*(75%)–*endo*(25%) monomer mixture of *N*-phenyl-norbornene-5,6-dicarboximide (**1b**) were prepared as described previously [14,18]. Norbornene (**NB**), phenol and sodium 4-hydroxybenzenesulfonate dihydrate were purchased from Aldrich Chemical Co. and used without further purification. 1,2-Dichloroethane, dichloromethane, *p*-dioxane, toluene and *N,N*-dimethylacetamide were dried over anhydrous calcium chloride and distilled over CaH₂. Bis(tricyclohexylphosphine)benzylideneruthenium(IV) dichloride (**I**), tricyclohexylphosphine [1,3-bis(2,4,6-trimethylphenyl)-4,5-dihydroimidazol-2-ylidene][benzylidene] ruthenium dichloride (**II**) and ClRh(PPh₃)₃ were purchased from Aldrich Chemical Co. and used as received.

2.3. Metathesis copolymerization of monomers

Copolymerizations were carried out in glass vials under dry nitrogen atmosphere. They were quenched by adding a small amount of ethyl vinyl ether and the solutions were poured into an excess of methanol. The copolymers were purified by solubilization in chloroform and precipitation into methanol containing a few drops of 1 N HCl. The obtained copolymers were dried in a vacuum oven at 40 °C to constant weight.

2.3.1. Synthesis of random poly(*N*-pentafluorophenyl-norbornene-5,6-dicarboximide-co-*N*-phenyl-norbornene-5,6-dicarboximide) (**2**)

Monomer **1a** (0.50 g, 1.51 mmol) and monomer **1b** (0.36 g, 1.51 mmol) were initially dissolved in 4.34 mL of 1,2-dichloroethane. Then catalyst **I** (2.49 × 10⁻³ g, 0.0030 mmol) was added and the mixture was stirred at 65 °C for 2 h (Scheme 1). The obtained copolymer **2** was soluble in chloroform and dichloroethane: Incorporation of **1a** in copolymer = 48 mol%; *M*_n = 2.85 × 10⁵; *M*_w/*M*_n = 1.22; *T*_g = 205 °C; *T*_d = 425 °C; ¹H NMR (300 MHz, CDCl₃): δ (ppm) = 7.45–7.23 (5H, m), 5.78 (2H, s, *trans*), 5.56 (2H, s, *cis*), 3.23–3.15 (4H, s), 2.87 (4H, s), 2.21 (2H, s), 1.73 (2H, s); ¹³C NMR (75 MHz, CDCl₃): δ (ppm) = 177.0 (C=O), 174.8 (C=O),



Scheme 1. Synthesis of polynorbornene based copolymers via ROMP.

145.1–139.6 (C–F), 136.2 (*cis*), 131.7 (*trans*), 129.0, 126.3, 107.2, 50.9, 46.1, 41.6; ^{19}F NMR (282 MHz, CDCl_3 , ref. TFA [–77ppm]): δ (ppm) = –142.1, –142.5, –143.1, –150.0, –150.4, –159.7, –160.0; FT-IR (thin film, cm^{-1}): 3018, 2923 (C–H asym str), 2853 (C–H sym str), 1777 (C=O), 1706 (C=O), 1598 (C=C str), 1514, 1455 (C–N), 1356, 1297 (C–F), 1165, 1139, 1066, 1021, 985, 880, 785, 768, 746, 690.

2.3.2. Synthesis of block poly(*N*-pentafluorophenyl-norbornene-5,6-dicarboximide-co-*N*-phenyl-norbornene-5,6-dicarboximide) (**3**)

Monomer **1b** (0.36 g, 1.51 mmol) and catalyst **I** (2.49×10^{-3} g, 0.0030 mmol) were stirred in 2.17 mL of 1,2-dichloroethane at 65 °C for 0.33 h. Then, 0.50 g (1.51 mmol) of monomer **1a** dissolved in 2.17 mL of 1,2-dichloroethane was added to the polymer solution and stirred at 65 °C for 0.66 h (Scheme 1). The obtained copolymer **3** was soluble in chloroform and dichloroethane: Incorporation of **1a** in copolymer = 32 mol%; $M_n = 2.60 \times 10^5$; $M_w/M_n = 1.15$; $T_{g1} = 170$ °C; $T_{g2} = 224$ °C; $T_d = 424$ °C; ^1H NMR (300 MHz, CDCl_3): δ (ppm) = 7.44–7.24 (5H, m), 5.77 (2H, s, *trans*), 5.55 (2H, s, *cis*), 3.25–3.14 (4H, s), 2.87 (4H, s), 2.20 (2H, s), 1.68 (2H, s); ^{13}C NMR (75 MHz, CDCl_3): δ (ppm) = 177.1 (C=O), 174.7 (C=O), 144.9–139.4 (C–F), 132.1 (*cis*), 131.9 (*trans*), 129.0, 126.6, 107.5 (C–N), 50.9, 46.1, 41.7; ^{19}F NMR (282 MHz, CDCl_3 , ref. TFA [–77ppm]): δ (ppm) = –142.2, –142.7, –143.2, –150.0, –150.3, –159.7, –160.0, –160.7; FT-IR (thin film, cm^{-1}): 3022, 2925 (C–H asym str), 2838 (C–H sym str), 1774 (C=O), 1707 (C=O), 1588 (C=C str), 1517, 1455 (C–N), 1360, 1299 (C–F), 1167, 1022, 988, 746, 690.

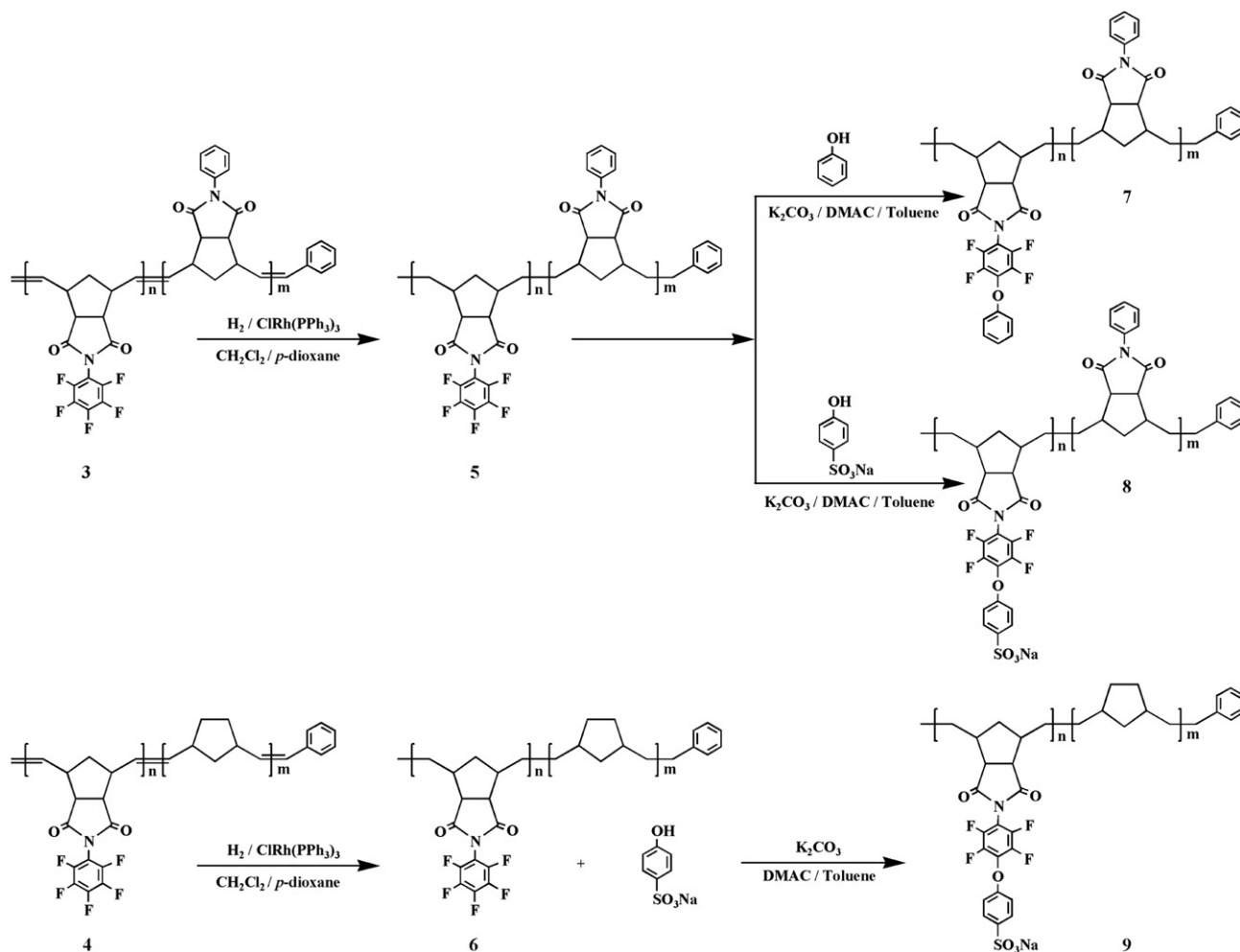
2.3.3. Synthesis of block poly(*N*-pentafluorophenyl-norbornene-5,6-dicarboximide-co-Norbornene) (**4**)

Monomer **1a** (0.50 g, 1.51 mmol) and catalyst **I** (2.49×10^{-3} g, 0.0030 mmol) were stirred in 2.5 mL of 1,2-dichloroethane at 45 °C for 0.5 h. Then, 0.14 g (1.51 mmol) of norbornene dissolved in 3.5 mL of 1,2-dichloroethane was added to the polymer solution and stirred

at 45 °C for 0.16 h (Scheme 1). The obtained copolymer **4** was soluble in chloroform and dichloroethane: Incorporation of **1a** in copolymer = 49 mol%; $M_n = 2.11 \times 10^5$; $M_w/M_n = 1.25$; $T_{g1} = 44$ °C; $T_{g2} = 170$ °C; $T_d = 420$ °C; ^1H NMR (300 MHz, CDCl_3): δ (ppm) = 5.77 (1H, s, *trans*), 5.55 (1H, s, *cis*), 5.34 (1H, m, *trans*), 5.22 (1H, m, *cis*), 3.27 (2H, s), 2.88 (2H, s), 2.44–2.22 (2H, m), 1.92–1.02 (8H, m); ^{13}C NMR (75 MHz, CDCl_3): δ (ppm) = 174.5 (C=O), 147.1–141.2 (C–F), 135.2, 133.7 (*cis*), 133.3 (*cis*), 132.5 (*trans*); 131.9 (*trans*), 107.3 (C–N), 51.2, 46.7, 43.1, 41.8, 40.5, 32.1; ^{19}F NMR (282 MHz, CDCl_3 , ref. TFA [–77ppm]): δ (ppm) = –142.2, –142.6, –143.1, –150.1, –150.3, –159.8, –160.1, –160.7; FT-IR (thin film, cm^{-1}): 3008, 2932 (C–H asym str), 2859 (C–H sym str), 1795 (C=O), 1727 (C=O), 1650 (C=C str), 1513, 1452, 1370, 1356, 1294 (C–F), 1165, 1138, 984, 785, 767, 624.

2.4. Hydrogenation of **3**

0.5 g of **3** was added to 60 mL of solvent (dichloromethane-*p*-dioxane, 1:1) in a Schlenk tube. Wilkinson's catalyst, $\text{ClRh}(\text{PPh}_3)_3$, (5 wt%) was previously introduced into a Parr shaker reactor. The solution was degassed and charged into the reactor under N_2 . Then hydrogen was added. A 99% of hydrogenation, determined by ^1H NMR, for **5** was achieved using a Wilkinson's catalyst, $\text{ClRh}(\text{PPh}_3)_3$, at room temperature and 115 bar (Scheme 2). The obtained polymer **5** was soluble in chloroform and dichloromethane. Incorporation of **1a** in copolymer = 32 mol%; $T_{g1} = 143$ °C; $T_{g2} = 198$ °C; $T_d = 460$ °C; ^1H NMR (300 MHz, CDCl_3): δ (ppm) = 7.48–7.23 (5H, m), 3.03–2.93 (2H, m), 2.17, 1.89, 1.60, 1.23; ^{13}C NMR (75 MHz, CDCl_3): δ (ppm) = 177.9 (C=O), 175.6 (C=O), 144.7–139.1 (C–F), 131.8, 128.9, 128.3, 126.4, 107.4 (C–N), 51.9, 44.0, 42.1, 33.7; ^{19}F NMR (282 MHz, CDCl_3 , ref. TFA [–77ppm]): δ (ppm) = –142.2, –143.1, –150.2, –150.3, –159.8, –160.2; FT-IR (thin film, cm^{-1}): 2923 (C–H asym str), 2846 (C–H sym str), 1779 (C=O), 1706 (C=O), 1517, 1456 (C–N), 1359, 1299, (C–F), 1168, 1036, 988.



Scheme 2. Hydrogenation and further aromatic substitution of polynorbornene based copolymers bearing pentafluorophenyl moieties.

2.5. Hydrogenation of **4**

0.5 g of **4** was added to 60 mL of solvent (dichloromethane-*p*-dioxane, 1:1) in a Schlenk tube. Wilkinson's catalyst, $\text{CIRh}(\text{PPh}_3)_3$, (5 wt%) was previously introduced into a Parr shaker reactor. The solution was degassed and charged into the reactor under N_2 . Then hydrogen was added. A 98% of hydrogenation, determined by ^1H NMR, for **6** was achieved using a Wilkinson's catalyst, $\text{CIRh}(\text{PPh}_3)_3$, at room temperature and 115 bar (Scheme 2). The obtained polymer **6** was soluble in chloroform and dichloromethane. Incorporation of **1a** in copolymer = 49 mol%; $T_{g1} = 4^\circ\text{C}$; $T_{g2} = 143^\circ\text{C}$; $T_d = 454^\circ\text{C}$; ^1H NMR (300 MHz, CDCl_3): δ (ppm) = 3.06 (2H, s), 2.30–1.25 (20H, m); ^{13}C NMR (75 MHz, CDCl_3): δ (ppm) = 174.6 (C=O), 147.0–141.3 (C–F), 135.2, 107.4 (C–N), 51.1, 46.6, 43.1, 41.7, 40.6, 32.2; ^{19}F NMR (282 MHz, CDCl_3 , ref. TFA [-77ppm]): δ (ppm) = -142.2, -142.5, -143.1, -150.1, -150.5, -159.8, -160.1, -160.4; FT-IR (thin film, cm^{-1}): 3012, 2937 (C–H asym str), 2862 (C–H sym str), 1796 (C=O), 1723 (C=O), 1510, 1456, 1378, 1360, 1293 (C–F), 1169, 1135, 986, 785, 767, 620.

2.6. Synthesis of **7**

Hydrogenated poly(*N*-pentafluorophenyl-*exo-endo*-norbornene-5,6-dicarboximide-*co-N*-phenyl-*exo-endo*-norbornene-5,6-dicarboximide) (**5**) (1.0 g, 1.74 mmol), phenol (0.25 g, 2.62 mmol) and potassium carbonate (0.44 g, 3.18 mmol) were mixed in a round flask equipped with a Dean–Stark trap and stirred in 18 mL of solvent

(*N,N*-dimethylacetamide-toluene, 10:1) at 120°C for 3 h (Scheme 2). Progressive precipitation overtime was observed. The product was then filtered off, washed several times with distilled water and dried in a vacuum oven at 40°C overnight. The resulting polymer **7**, a dark-brown powder, was soluble in DMSO. Incorporation of **1a** in copolymer = 32 mol%; Yield: 94%; $T_{g1} = 180^\circ\text{C}$; $T_{g2} = 198^\circ\text{C}$; $T_d = 456^\circ\text{C}$; ^1H NMR (300 MHz, $\text{DMSO}-d_6$): δ (ppm) = 7.51–6.92 (10H, m), 3.64 (2H, s), 3.10, 2.22, 1.91, 1.63, 1.26; ^{13}C NMR (75 MHz, $\text{DMSO}-d_6$): δ (ppm) = 178.3 (C=O), 177.7 (C=O), 127.6 (C–O), 114.8, 107.3 (C–N), 51.4; FT-IR (thin film, cm^{-1}): 3423, 2927 (C–H asym str), 2850 (C–H sym str), 1707 (C=O), 1693 (C=O), 1684, 1506, 1494, 1357, 1294 (C–F), 1120, 1010, 981, 743, 689, 607.

2.7. Synthesis of **8**

Hydrogenated poly(*N*-pentafluorophenyl-*exo-endo*-norbornene-5,6-dicarboximide-*co-N*-phenyl-*exo-endo*-norbornene-5,6-dicarboximide) (**5**) (1.0 g, 1.74 mmol), sodium 4-hydroxybenzenesulfonate dihydrate (0.61 g, 2.62 mmol) and potassium carbonate (0.44 g, 3.18 mmol) were mixed in a round flask equipped with a Dean–Stark trap and stirred in 22 mL of solvent (*N,N*-dimethylacetamide-toluene, 10:1) at 120°C for 5 h (Scheme 2). Progressive precipitation overtime was observed. The product was then filtered off, washed several times with distilled water and dried in a vacuum oven at 40°C overnight. The resulting polymer **8**, a pale-brown powder, was soluble in DMF and DMSO. Incorporation of **1a** in copolymer = 32 mol%; Yield: 96%;

$T_{g1} = 198$ °C; $T_{g2} = 227$ °C; $T_{d1} = 272$ °C (sulfonic group loss); $T_{d2} = 458$ °C (main chain decomposition); $^1\text{H NMR}$ (300 MHz, DMF- d_7): δ (ppm) = 7.81 (2H, m), 7.53–7.34 (5H, m), 7.27 (2H, m), 3.65 (2H, s), 3.09, 2.24, 1.90, 1.65, 1.28; $^{13}\text{C NMR}$ (75 MHz, DMSO- d_6): δ (ppm) = 178.2 (C=O), 177.9 (C=O), 127.9 (C–O), 114.9, 107.5 (C–N), 51.6; $^{19}\text{F NMR}$ (282 MHz, DMF- d_7 , ref. TFA [-77ppm]): δ (ppm) = -141.9, -142.9, -150.0, -153.1, -160.4; FT-IR (thin film, cm^{-1}): 3420, 2923 (C–H asym str), 2854 (C–H sym str), 1703 (C=O), 1698 (C=O), 1682, 1505, 1492, 1359, 1291 (C–F), 1165 (–SO₃H, asym str), 1124, 1033 (–SO₃H, sym str), 1008, 987, 742, 689, 608.

2.8. Synthesis of **9**

Hydrogenated poly(*N*-pentafluorophenyl-*exo-endo*-norbornene-5,6-dicarboximide-*co*-Norbornene) (**6**) (1.0 g, 2.34 mmol), sodium 4-hydroxybenzenesulfonate dihydrate (0.81 g, 3.48 mmol) and potassium carbonate (0.59 g, 4.27 mmol) were mixed in a round flask equipped with a Dean–Stark trap and stirred in 26 mL of solvent (*N,N*-dimethylacetamide-toluene, 10:1) at 120 °C for 5 h (Scheme 2). Progressive precipitation overtime was observed. The product was then filtered off, washed several times with distilled water and dried in a vacuum oven at 40 °C overnight. The resulting polymer **9**, a dark-brown powder, was soluble in DMSO. Incorporation of **1a** in

copolymer = 49 mol%; Yield: 95%; $T_{g1} = 4$ °C; $T_{g2} = 227$ °C; $T_{d1} = 268$ °C (sulfonic group loss); $T_{d2} = 448$ °C (main chain decomposition); $^1\text{H NMR}$ (300 MHz, DMSO- d_6): δ (ppm) = 7.68 (2H, s), 7.19 (2H, s), 3.26 (2H, s), 2.11–1.22 (20H, m); $^{13}\text{C NMR}$ (75 MHz, DMSO- d_6): δ (ppm) = 174.7 (C=O), 135.2, 128.1 (C–O), 107.3 (C–N), 51.1, 46.3, 43.2, 41.5, 40.5, 32.3; $^{19}\text{F NMR}$ (282 MHz, DMSO- d_6 , ref. TFA [-77ppm]): δ (ppm) = -142.3, -143.3, -150.2, -153.2, -160.3; FT-IR (thin film, cm^{-1}): 3480, 2932 (C–H asym str), 2870 (C–H sym str), 1798 (C=O), 1725 (C=O), 1680, 1515, 1494, 1357, 1299 (C–F), 1260, 1168 (–SO₃H, asym str), 1139, 1032 (–SO₃H, sym str), 987, 802, 767, 696.

2.9. Density, water uptake and ion-exchange capacity

The density of the dry membrane of copolymer **8** was measured by the flotation method using isoctane as solvent. The value of this parameter is $\rho = 1380$ kg m⁻³.

Weighed dry membranes from copolymer **8** were immersed and kept in deionized distilled water overnight. The membranes were removed from water, gently blotted with filter paper to remove surface water and weighed. This operation was repeated three times. Water uptake was obtained by means of the expression

$$\text{Water uptake} = \frac{\text{weight wet membrane} - \text{weight dry membrane}}{\text{weight dry membrane}} \times 100 \quad (1)$$

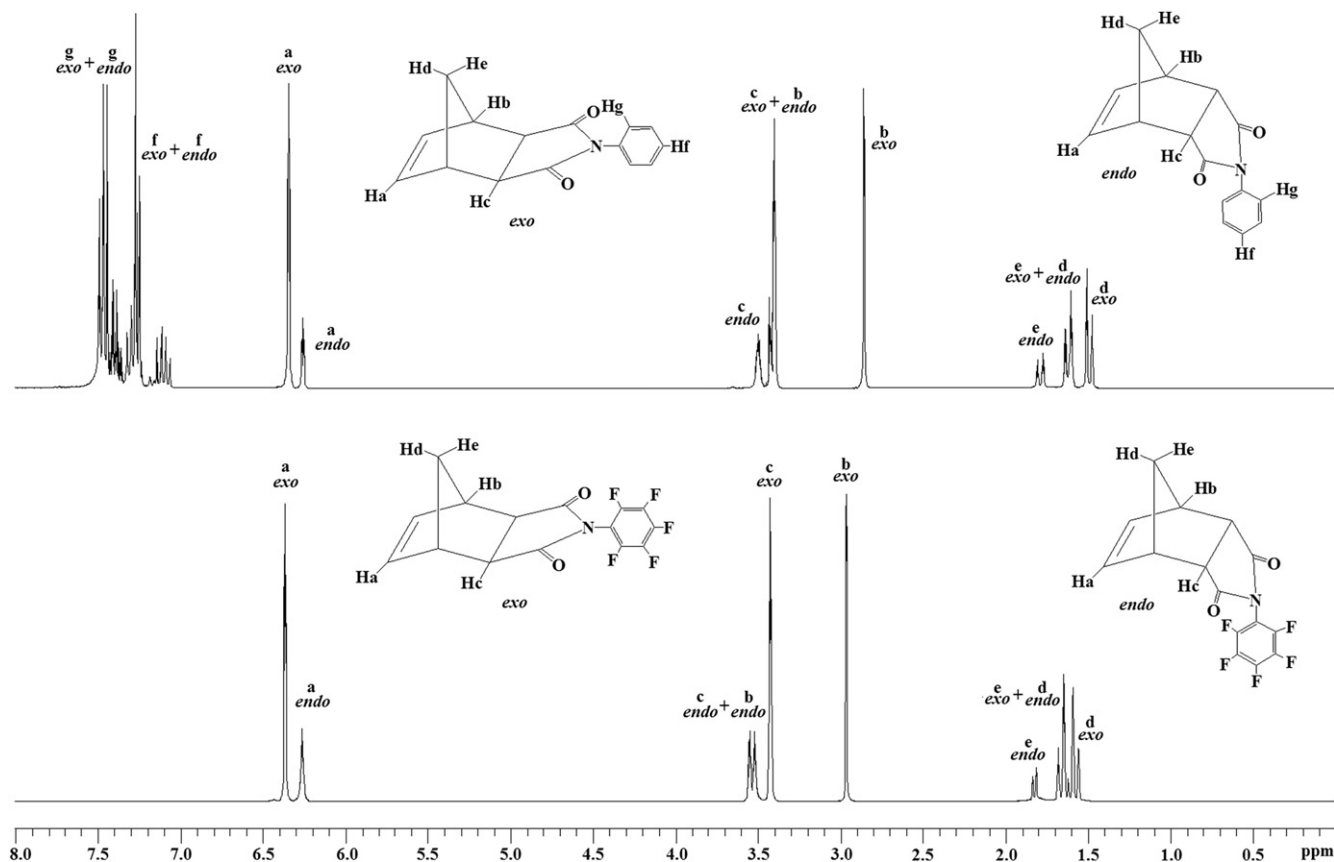


Fig. 1. $^1\text{H NMR}$ spectra of *exo*(75%)-*endo*(25%) monomer mixtures of **1a** (bottom) and **1b** (top).

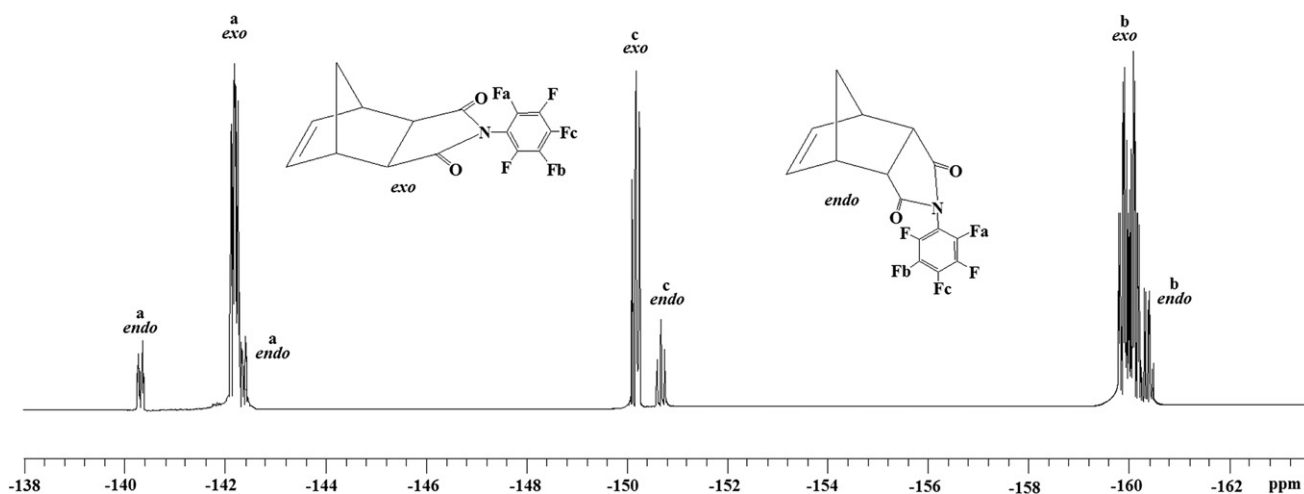
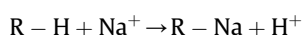


Fig. 2. ^{19}F NMR spectrum of *exo*(75%)-*endo*(25%) monomer mixture of **1a**.

To evaluate the ion-exchange capacity, the membranes in the acid form were equilibrated with a NaCl solution 1M, after the hydrochloric acid was liberated in the interchange reaction



the pH of the acid solution was measured. The values of the ion-exchange capacity (IEC) and the water uptake (w_{u}) are, respectively, 0.286 eq/kg dry membrane and 0.373 kg H_2O /kg dry membrane. The theoretical value of IEC is of 0.204 eq/kg dry membrane.

2.10. Electromotive force of concentration cells

The electromotive force of the concentration cell with configuration Ag|AgCl| electrolyte concentration (m_1) |cation-exchange membrane| electrolyte concentration (m_2)| AgCl|Ag, where m represents the molal concentration, was measured with a Hioki potentiometer, at 25 °C, for various concentrations of hydrochloric acid and sodium chloride solutions, respectively. Electromotive forces were monitored as a function of time via a PC. The ratio of the molal concentrations m_2/m_1 was kept in the vicinity of 2 in all the cases.

2.11. Ohmic resistance measurements

The ohmic resistance of the membrane in the acid form was measured with a Novocontrol BDS system comprising a frequency response analyzer (Solartron Schlumberger FRA 1260) and a broadband dielectric converter with an active sample head. Gold disk electrodes were used in the impedance measurements carried out at several temperatures in the frequency window 4.9×10^{-2} – 3×10^6 Hz. The temperature was controlled by a nitrogen jet (QUATRO from Novocontrol) with a temperature error of 0.1 K during every single sweep in frequency.

3. Results and discussion

The ^1H NMR spectra of these norbornene dicarboximides show signals with rather similar relative intensities and chemical shifts. The *exo* and *endo* olefinic signals of **1a** and **1b** were well-resolved in both ^1H NMR spectra and appeared as singlets in the region of 6.5–6.0 ppm (Fig. 1). From the relative intensities of these signals the ratio of *exo* and *endo* isomers was determined to be 75:25. The other signals showed overlapping owing to the presence of the

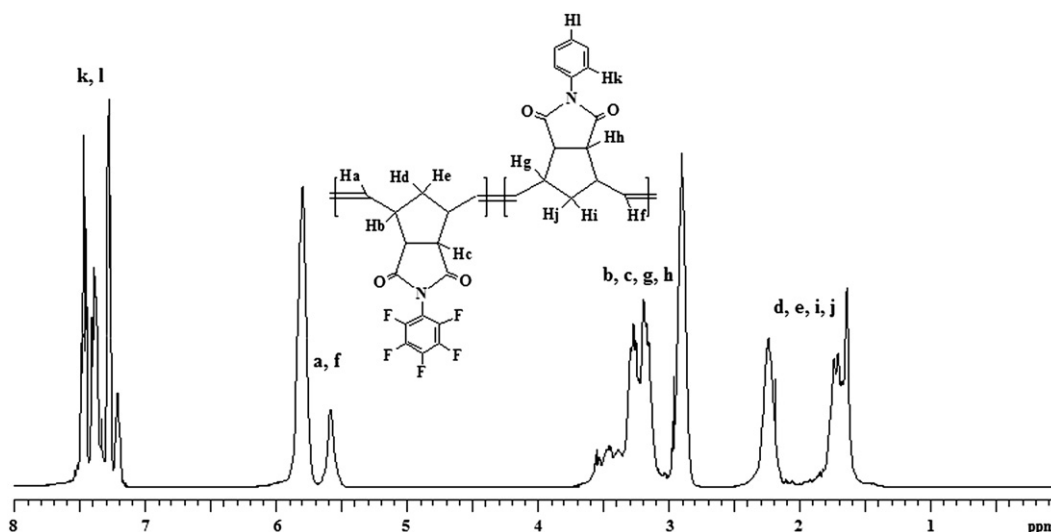


Fig. 3. ^1H NMR spectrum of copolymer **2**.

Table 1
Copolymerization conditions of monomers **1a** and **1b** for reactivity constants determination.

Entry	Mass of 1a in the feed (g)	Mol % of 1a in the feed ^a	Incorporation of 1a in copolymer (%) ^b	Time (s)	Yield (%) ^c
1	0.3	20	7.9	25	14.1
2	0.3	40	23.4	25	08.9
3	0.5	50	29.6	25	15.0
4	0.3	60	41.9	30	12.2
5	0.5	80	66.6	30	07.4

^a Molar ratio of monomer to catalyst = 1000, 1,2-Dichloroethane as solvent, temperature = 65 °C, Initial monomer concentration [M₀] = 0.7 mol/L.

^b Determined by ¹H NMR.

^c Methanol insoluble polymer.

minor isomer, mainly in the methylene and aromatic proton regions, and an accurate integration could not be made.

The ¹⁹F NMR spectrum of **1a** shown in Fig. 2 displays, on one hand, three major signals corresponding to the *exo* isomer, that for –F in *ortho* position occurs at –142.2 ppm, that for –F in *meta* position between –159.7 and –160.2 ppm and that for –F in *para* position appears at –150.1 ppm. On the other hand, four minor signals corresponding to the *endo* isomer are observed and assigned as follows: those for –F in *ortho* position occur at –140.3 ppm and –142.3 ppm, that for –F in *meta* position appears at –160.4 ppm and that for –F in *para* position occurs at –150.6 ppm. Based on the *exo* and *endo* signals of the fluorine atom in *para* position, which appear at –150.1 ppm and –150.6 ppm respectively, the *exo:endo* ratio of **1a** was also determined from the ¹⁹F NMR spectrum being consistent with those ratios obtained from other signal integrations as well as with the previous determinations made by ¹H NMR spectroscopy.

Copolymerizations of **1a** and **1b**, for reactivity constants determination, were carried out in 1,2-dichloroethane at 65 °C, via ROMP, using bis(tricyclohexylphosphine)benzylidene ruthenium(IV) dichloride (**I**) (Scheme 1). The reactions were conducted at 20, 40, 50, 60 and 80 mol percent of monomer **1a** in the feed and quenched before a 15 weight percent of monomer conversion was

reached. ¹H NMR was used to determine the incorporation of **1a** in the different copolymers synthesized (Fig. 3) by integrating the area of the olefinic proton region ($\delta = 5.5\text{--}5.8$ ppm) relative to aromatic proton region ($\delta = 7.1\text{--}7.4$ ppm). Table 1 summarizes the results of the copolymerizations of **1a** and **1b**. Since at the conversion desired (≤ 15 wt%) monomer **1a** was not detected in the copolymer formed when the reactions were conducted at 45 °C, the experiments for reactivity constant determination were carried out at 65 °C and incorporation of monomer **1a** could be successfully quantified by ¹H NMR. Furthermore, as mol percent of **1a** in the feed was increased, more reaction time was needed for copolymerization to take place until the conversion desired (Table 1, entries 4 and 5). It has been previously indicated that the more *endo* isomer in the mixture feed the lower level of activity that is displayed by **I** at 45 °C [18]. Up to now, research is being carried out to clarify what causes this very low catalytic activity in the presence of **1a** at 45 °C, a temperature typically used for the ROMP of norbornene dicarboximides. On the basis of the results obtained from the copolymerization experiments, the reactivity constants **r**_{1a} and **r**_{1b} were determined by using the general copolymerization equation. By applying the Mayo-Lewis method [19] the values obtained were **r**_{1a} = 0.601 and **r**_{1b} = 4.235 whereas by applying the Fineman-Ross method [20] the values obtained were **r**_{1a} = 0.449 and **r**_{1b} = 3.728 for monomer **1a** and **1b**, respectively. The precision of experimentally determined monomer reactivity ratios depends on the experimental design and technique used to analyze the data. Results obtained for acrylamide monomer by applying the Mayo-Lewis and Fineman-Ross methods, for example, are reported to vary up to 58% from each other [21]. It is worth noting that these linear methods are used only to give preliminary estimates of reactivity ratios which are used in nonlinear methods to generate more accurate results.

Block and random high molecular weight copolymers were also synthesized via ROMP using bis(tricyclohexylphosphine)benzylideneruthenium(IV) dichloride (**I**) and tricyclohexylphosphine [1,3-bis(2,4,6-trimethylphenyl)-4,5-dihydroimidazol-2-ylidene]benzylidene]ruthenium dichloride (**II**) (Scheme 1). Table 2 summarizes

Table 2
General conditions for copolymerization of monomer **1a** with **1b** and norbornene (**NB**), respectively.

Entry	Comonomer	Fashion	Catalyst ^a	[M ₀] (mol/L)	Temperature (°C)	Time (min)	Incorporation of 1a in copolymer (%) ^b	Yield (%) ^c	M _n × 10 ^{-5d}	MWD ^d
1	1b	Random	II	1.0	25	5	42	91	2.45	1.26
2	1b	Random	II	0.5	25	240	44	97	2.79	1.38
3	1b	Random	I	0.7	45	5	–	14	0.35	1.24
4	1b	Random	I	0.7	45	15	30	65	1.53	1.17
5	1b	Random	I	0.7	45	60	39	81	2.20	1.19
6	1b	Random	I	0.7	45	120	43	89	2.22	1.20
7	1b	Random	I	0.7	65	120	48	97	2.85	1.22
8	1b	Block	I	0.7	65	20 ^e 40 ^f	32	84	2.60	1.15
9	1b	Block	I	0.7	65	20 ^e 60 ^f	41	88	2.73	1.16
10	1b	Block	I	0.7	65	20 ^e 80 ^f	48	96	2.80	1.20
11	NB	Block	I	0.5	25	20 ^f 10 ^g	21	57	1.12	1.24
12	NB	Block	I	0.5	45	20 ^f 10 ^g	38	83	1.87	1.23
13	NB	Block	I	0.5	45	30 ^f 10 ^g	49	98	2.11	1.25

^a Molar ratio of monomer to catalyst = 1000, 1,2-Dichloroethane as solvent, Mol % of **1a** in the feed = 50.

^b Determined by ¹H NMR.

^c Methanol insoluble polymer.

^d GPC analysis in tetrahydrofuran with polystyrene calibration standards.

^e Reaction time for monomer **1b**.

^f Reaction time for monomer **1a**.

^g Reaction time for **NB**.

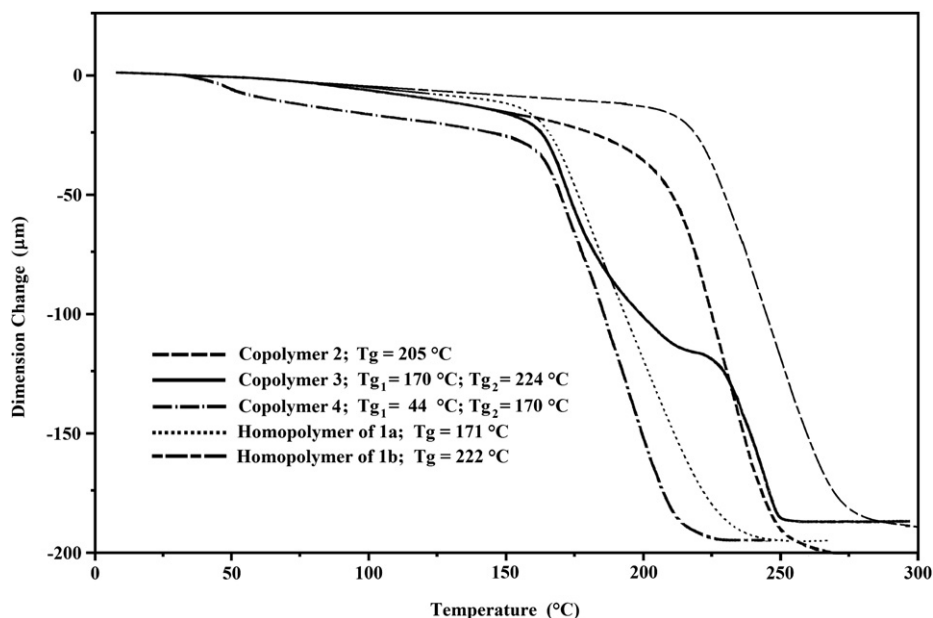


Fig. 4. Thermomechanical analysis of random copolymer **2**, block copolymer **3**, block copolymer **4**, homopolymer of **1a** and homopolymer of **1b**, respectively.

the results of the high conversion copolymerizations of **1a** with **1b** and **NB**, respectively. It is observed that catalyst **II** produced random high molecular weight copolymers in the early minutes of reaction in high yield at room temperature with almost complete incorporation of **1a** in the copolymer (Entry 1). On the contrary, catalyst **I** was not able to incorporate monomer **1a** in copolymer in the same time even at 45 °C (Entry 3) and more reaction time was needed for the incorporation of **1a** to take place and it could be detected by ^1H NMR (Entries 4 and 5). For the same period of time (120 min), quantitative incorporation of monomer **1a** in copolymer, in high yield and using catalyst **I**, was achieved when the polymerization was conducted at 65 °C rather than 45 °C (Entries 6 and 7). Block copolymers of **1a** with **1b** and **NB** were synthesized in high yields using catalyst **I** (Entries 8–13). In the first case, the copolymerizations were conducted at 65 °C and the monomer **1b** was added initially polymerizing completely within 0.33 h (Entries 8–10). Immediately, monomer **1a** was added to the reaction and quantitative incorporation of **1a** in copolymer was detected after 1.33 h of being added to the growing polymer (Entry 10). In the second case, monomer **1a** was added firstly and allowed to polymerize during 0.5 h. Then, **NB** was added to the reaction and after 0.16 h the copolymerization was inhibited. Quantitative incorporation of **1a** in copolymer was detected when the copolymerization was conducted at 45 °C (Entry 13). Compared to *exo*-monomer where functional groups are far from the metal active center the polar groups of *endo*-monomer may coordinate to the

metallacarbene active center inhibiting the polymerization. A coordination of the ruthenium atom to the fluorine atom of the perfluoroaromatic moiety of the *endo*-monomer of **1a** is possible in a similar way that the ruthenium atom is coordinated to the sulfur atom of certain olefin metathesis initiators bearing sulfoxide moieties which have exhibited poor activity at room temperature but a reasonable and increased level of activity at elevated temperatures. These complexes seemed to be dormant at low temperature on the contrary the catalysis proceeded quickly when the temperature was raised [22]. We consider that the least active catalyst **I** (in comparison with catalyst **II**), the Ru-fluorine intramolecular interaction and the steric effect of the pentafluorinated ring in *endo*-monomer of **1a** are factors which difficult the complete incorporation of the monomer **1a** in the copolymer using **I**. Fig. 4 shows the thermomechanical analysis performed on the random and block copolymers synthesized as well as those of the corresponding homopolymers of **1a** and **1b** used as references, respectively. As expected, a single transition is observed, at 205 °C, and interpreted as the glass transition temperature, T_g , of the random copolymer **2** whereas two transitions are observed for the block copolymer **3**, at 170 °C and 224 °C, and attributed to the corresponding T_g of **1a** and **1b** homopolymer regions, respectively. Similarly, two transitions are also observed for the block copolymer **4**, at 44 °C and 170 °C, which were interpreted as the T_g of **NB** and **1a** homopolymer regions, respectively. Furthermore, the thermo-oxidative stabilities of block copolymers **3** and **4** were enhanced

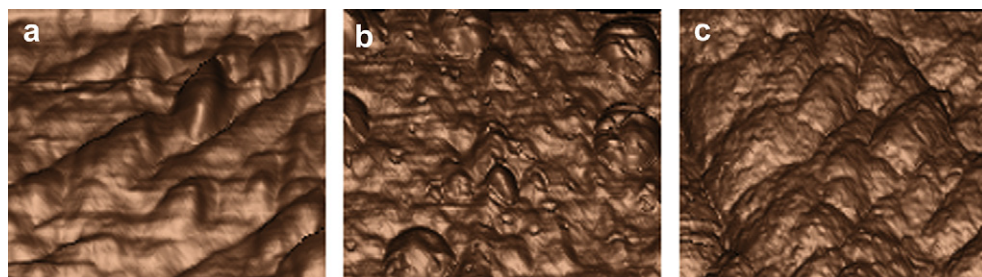


Fig. 5. 3-D AFM micrographs ($2 \times 2 \mu\text{m}$) of (a) block copolymer **3**, (b) hydrogenated copolymer **5** and (c) sulfonated copolymer **8**.

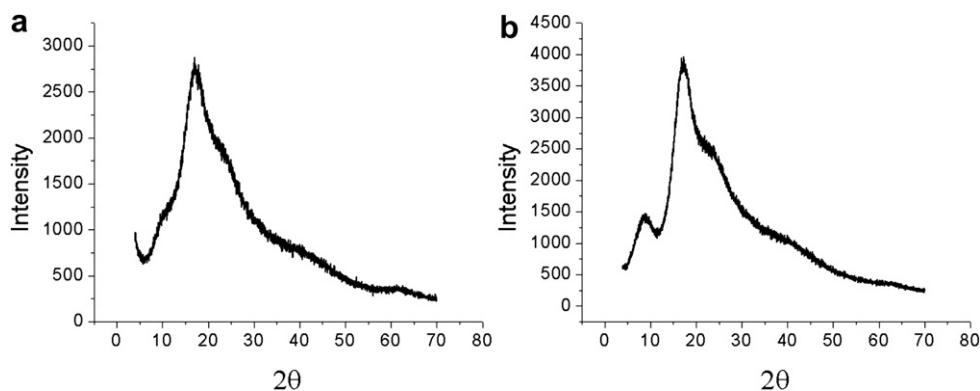


Fig. 6. X-Ray diffraction patterns of (a) random copolymer **2** and (b) block copolymer **3**.

by quantitative hydrogenations according to the methodology previously reported for these kinds of polymers (Scheme 2) [23]. In Fig. 5, the surface morphologies of (a) block copolymer **3**, (b) hydrogenated copolymer **5** and (c) dried sulfonated copolymer **8** are observed by tapping mode atomic force microscopy in three dimensions. The surface morphology in (a) shows an oriented morphological architecture characterized by broad peaks. This broadening could be attributed to the low surface energy of the pentafluorophenyl moieties which provide a thermodynamic driving force for the self-assembly at the surface air-polymer interface. In contrast, hydrogenation of the block copolymer seems to disturb the order generated by the presence of the double bonds and a much more disrupted surface is observed in (b). Finally, the surface morphology in (c) suggests that the sulfonic hydrophilic groups aggregate and, to a certain extent, phase separation begins to be noticeable. The presence of hydrophobic fluorine moieties affects the copolymer morphology in such a way that a surface enrichment of fluorine is generated. The latter assumption is commonly associated to a low surface energy. In fact, this effect of fluorine containing moieties in copolymers has also been observed for other fluorocopolymers of low-surface energy [24].

Fig. 6 shows the X-ray diffraction patterns of the as cast random copolymer **2** as well as block copolymer **3** films. Both copolymers show typical amorphous patterns with one broad diffraction peak with a maximum around 20° 2θ . Nevertheless, block copolymer **3**

exhibits another peak around 9° 2θ that can be attributed to different arrangements adopted by the fluorinated and non-fluorinated copolymer chain segments which seem to vanish after the hydrogenation step. It is worth noting that block copolymers are able to spontaneously assemble into a wide variety of nanostructures and spherical or cylindrical micelles, among other combinations [25].

Afterwards, we tested the reactivity of copolymer **5** in reaction with phenol (Scheme 2). The nucleophilic aromatic substitution reaction was quantitative demonstrating, in this manner, the tailorable functionality of the perfluorinated polynorbornene based copolymers. Once the phenoxy-derivative **7** was successfully obtained, we reacted the hydrogenated copolymers **5** and **6** with sodium 4-hydroxybenzenesulfonate dihydrate, following the procedure previously used for the sulfonation of hydrogenated poly(*N*-pentafluorophenyl-*exo-endo*-norbornene-5,6-dicarboximide) [18], and progressive precipitation of the ionomers overtime was observed (Scheme 2). Ionomer films were cast from sulfonated copolymer **8** and **9** solutions in DMF and DMSO, respectively. The films were quite flexible when fully hydrated and became somewhat brittle as they dried out. The ^{19}F NMR spectra of the hydrogenated copolymer **6** and the sulfonated copolymer **9** are very similar to the ^{19}F NMR spectra of copolymers **5** and **8**, shown in Fig. 7, respectively. According to Fig. 7, it is appreciated that the substitution reaction has taken place in the *para* position

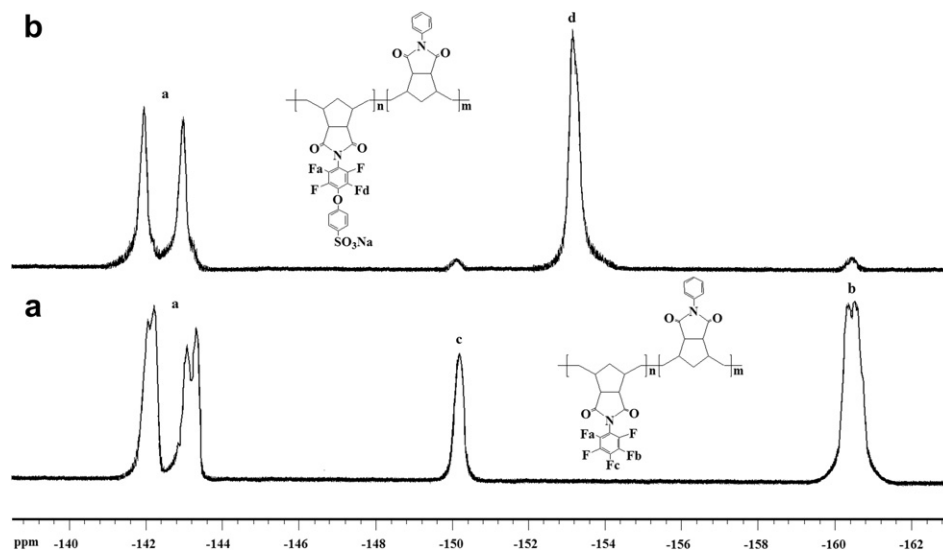


Fig. 7. ^{19}F NMR spectra of a) non-sulfonated copolymer **5** and b) sulfonated copolymer **8**.

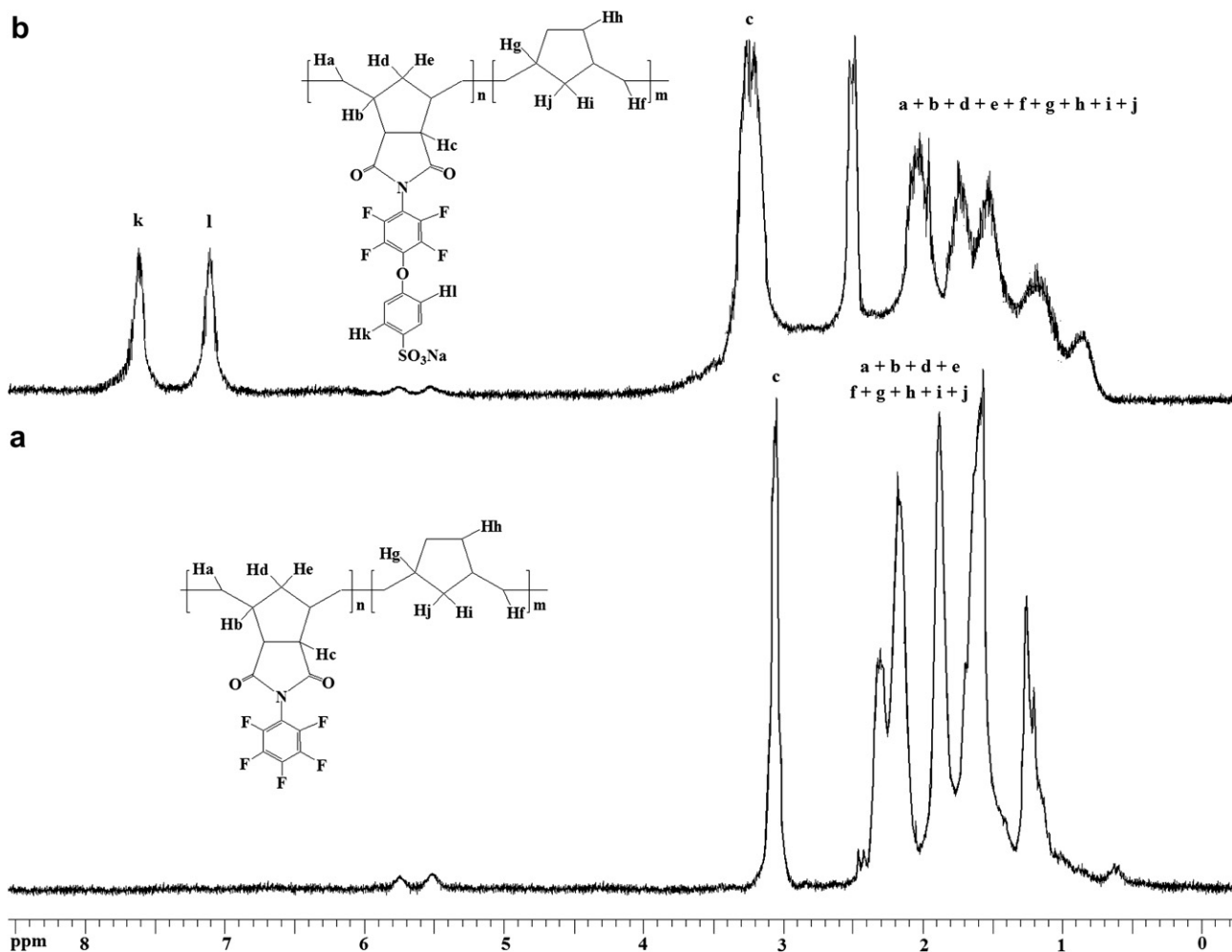


Fig. 8. ^1H NMR spectra of a) non-sulfonated copolymer **6** and b) sulfonated copolymer **9**.

(b, -150.1 ppm) since this signal has almost disappeared when a highly sulfonated copolymer is obtained. The ^1H NMR spectra of a) the saturated copolymer **6** and b) the sulfonated copolymer **9** are shown in Fig. 8. Clearly it is observed that the copolymer **6** has undergone a nucleophilic aromatic substitution due to the appearance of new signals at 7.68 ppm and 7.19 ppm assigned to the *meta* and *ortho* aromatic protons of the phenyl moiety bearing the sulfonate groups, respectively. In addition, FT-IR allowed us to confirm the introduction of sulfonate groups in the copolymers by observing the characteristic bands around 1033 and 1165 cm^{-1} assigned to symmetric and asymmetric stretching of sulfonate groups. The acid form copolymers **8** and **9** showed 5% weight losses of $268\text{ }^\circ\text{C}$ and $272\text{ }^\circ\text{C}$, respectively, which were assigned to the losses of the sulfonic groups whereas the second weight losses occurred at $448\text{ }^\circ\text{C}$ and $458\text{ }^\circ\text{C}$ were assigned to the thermal decompositions of the saturated main polymer chains. The mechanical properties of the copolymer **8** membrane were evaluated after soaking the film sample for 120 h at room temperature. The Young's modulus and the maximum stress were determined to be $E = 1615\text{ MPa}$ and $\sigma = 65\text{ MPa}$, respectively. The GPC analysis performed on the copolymers before and after being subjected to the sulfonation process do not show low molecular weight compounds. This indicates that the polymer chain scission, commonly caused by the hydrolysis of the imide ring in the main chain of linear polyimides, have not occurred during the sulfonation process of copolymer **8** which bears the imide moiety as a side chain group. The presence of hydrolysis products was neither able

to be detected by ^1H NMR. Copolymer **8** membranes in proton form ($100\text{--}150\text{ mg}$) aged in 500 mL of water at $90\text{ }^\circ\text{C}$ up to 72 h exhibited fairly good toughness level as they only broke when the films were hardly bent.

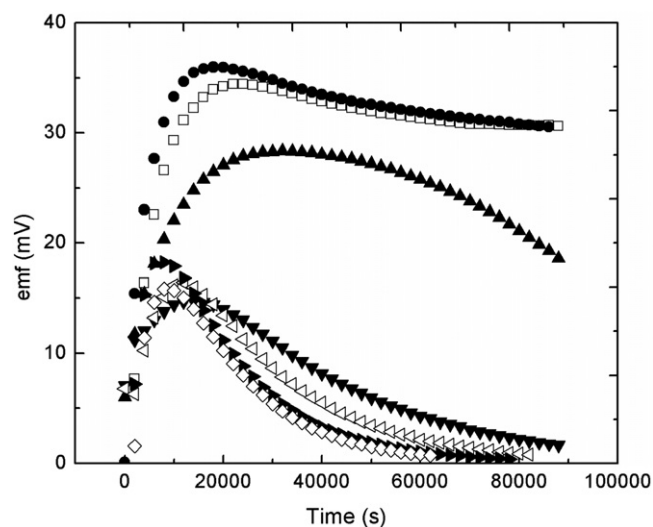


Fig. 9. Evolution of the emf of the copolymer **8** membrane for different c_2/c_1 ratios: (\square) 0.01/0.005, (\bullet) 0.02/0.01, (\blacktriangle) 0.1/0.05, (\blacktriangledown) 0.2/0.1, (\triangleleft) 0.4/0.2, (\blacktriangleright) 0.8/0.4, (\diamond) 1.0/0.5.

Table 3

Values of the hydrochloric acid concentration (molality), activity coefficient and electromotive force for the sulfonated copolymer **8** membrane.

m_1	m_2	γ_1	γ_2	emf (mV)
0.00519	0.01027	0.9263	0.9011	34.50
0.01027	0.02052	0.9011	0.8753	35.89
0.05072	0.10155	0.8324	0.7929	28.35
0.10167	0.20207	0.79287	0.76559	27.38
0.20218	0.40288	0.7655	0.7580	20.59
0.40288	0.79916	0.7580	0.7873	18.33
0.50522	0.99157	0.7579	0.8116	15.86

The replacement of the fluorine atom in *para* position of the pentafluorophenyl groups in the block hydrogenated poly(*N*-phenyl-*exo-endo*-norbornene-5,6-dicarboximide-*co-N*-pentafluorophenyl-*exo-endo*-norbornene-5,6-dicarboximide) using mild conditions yields an ionomer (**8**), thus opening new ways to the preparation of new polyelectrolytes. The permselectivity of cation-exchange membranes prepared from sulfonated copolymers with ion-exchange capacity 0.286 eq/kg was performed using concentration cells with configuration Ag|AgCl|electrolyte (m_1)|membrane|electrolyte (m_2)|AgCl|Ag. As electrolytes HCl and NaCl were used and the ratio of the molalities m_2/m_1 was roughly 2. The electromotive force (emf) of the concentration cell was measured under strong stirring in order to avoid polarization effects on the side of the membranes in contact with the electrolyte solutions. Prior to the experiments, the membrane was equilibrated with the less concentrated electrolyte solution. The membrane thickness was 50 μm . As can be seen in Fig. 9, the emf increases with time, initially rather fast until a maximum is reached, and then rather slowly, for the less concentrated solutions, and somewhat more rapidly, for the more concentrated solutions. The decrease is presumably caused by osmotic flow and free electrolyte diffusion that tend to decrease the m_2/m_1 ratio of the solutions. The emf at the maximum of the curve emf vs time was taken as the electromotive force of the concentration cell for the m_2/m_1 ratio of interest.

The sign of the emf changes when the concentrations in the compartments flanking the membrane are reversed. This behavior indicates that the cation-exchange membrane is symmetric. Values of the emf of the concentration cells for different m_2/m_1 concentration ratios are shown in Tables 3 and 4 for the HCl and NaCl electrolytes, respectively. As usual, the values of the emf decrease as the concentration of the electrolyte increases. It is worth noting that in spite of its relatively low IEC of 0.286 eq/kg dry membrane (the theoretical value of IEC is of 0.204 eq/kg dry membrane), the copolymer **8** membrane exhibits an unusual water uptake of 0.373 kg H₂O/kg dry membrane as well as a rather large number of molecules of water per fixed anionic group ($\lambda = 72.5$). This fact suggests that microphases separation in the latter membrane serves to compartmentalize an excess of water into the hydrophilic polar side chain domains, specifically in the vicinity of the dicarboximide side groups. For determining the experimental IEC, the sulfonated membrane was firstly soaked in

Table 4

Values of the sodium chloride concentration (molality), activity coefficient and electromotive force for the sulfonated copolymer **8** membrane.

m_1	m_2	γ_1	γ_2	emf (mV)
0.00509	0.01004	0.9318	0.9019	36.15
0.01004	0.02019	0.9019	0.8647	34.98
0.05008	0.10029	0.8180	0.7795	23.48
0.10029	0.19996	0.7795	0.7295	16.45
0.19996	0.39985	0.7295	0.6813	11.41
0.39985	0.79883	0.6813	0.6576	7.97
0.49994	1.00003	0.6704	0.6553	8.82

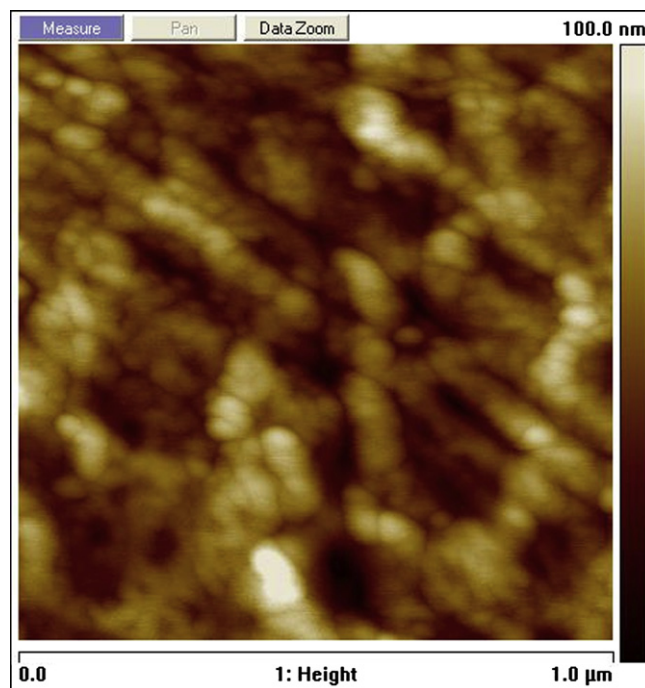


Fig. 10. AFM tapping phase image for the copolymer **8** membrane.

1.0 M HCl solution for 48 h to ensure the acid form of the membrane, and repeatedly washed with deionized water. Then, the membrane in the acid form was equilibrated with a NaCl solution 1M and after the hydrochloric acid was liberated in the interchange reaction the pH of the acid solution was measured. The slightly difference between the experimental and theoretical IECs could be attributed to residual HCl used to protonate the membrane which could be increasing the pH of the acid solution and therefore the experimental IEC. Fig. 10 shows the representative morphology of the copolymer **8** membrane. The molecular chains of this membrane contain respectively 68% and 32% molar fractions of phenyl and fluorinated pendant benzenesulfonate

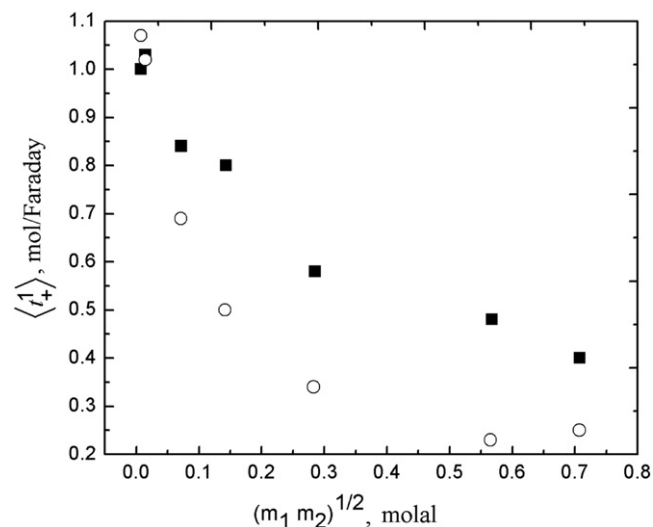


Fig. 11. Variation of the apparent proton (squares) and sodium cation (circles) transport numbers with the geometric average of the molality of the HCl and NaCl solutions flanking the membrane in copolymer **8**.

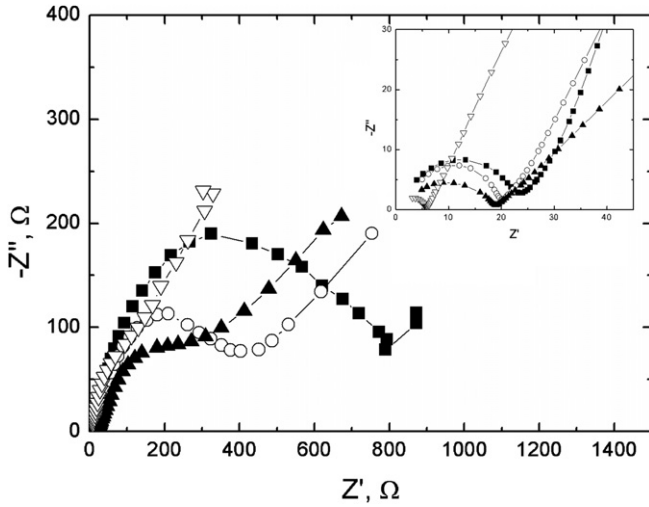


Fig. 12. Nyquist plots at 20 (■), 30 (○), 50 (▲) y 70 °C (▽) for the copolymer 8 membrane in the acid form equilibrated with distilled water. Inset: Zoom of the Nyquist plots at high frequencies. The curves were only used to connect the points.

moieties bonded to the dicarboximide side groups. It is expected that these moieties are mutually incompatible and therefore segregations occur giving rise to nano-size domains observed in the AFM of copolymer 8.

The following expression is applied for the electromotive force, E , measurements of the concentration cell of monovalent (1:1) electrolyte solutions [14]

$$E = -\frac{2RT}{F} \int_{a_1}^{a_2} t_+ d \ln a_2 = -\frac{2RT}{F} \bar{t}_+ \ln \frac{m_2 \gamma_2}{m_1 \gamma_1} \quad (2)$$

where F is Faraday's constant, γ_1 and γ_2 represent, respectively, the activity coefficients of the low and high concentration electrolyte solutions flanking the membranes in the concentration cell and \bar{t}_+ is the apparent counterion transport number in the membrane of the concentration cell.

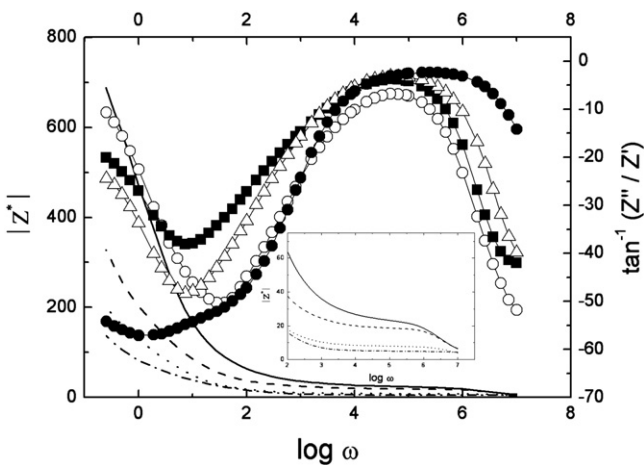


Fig. 13. Bode diagram showing the variation of the modulus of the impedance $|Z^*|$ (lines) and the out-of-phase angle ($\phi = \tan^{-1} Z''/Z'$) (symbols) with the frequency at 20 °C (solid line and filled circles), 40 °C (dash line and filled squares), 60 °C (dot line and open triangles) and 80 °C (dash dot line and filled circles) for the copolymer 8 membrane in the acid form equilibrated with distilled water. The curves were only used to connect the points.

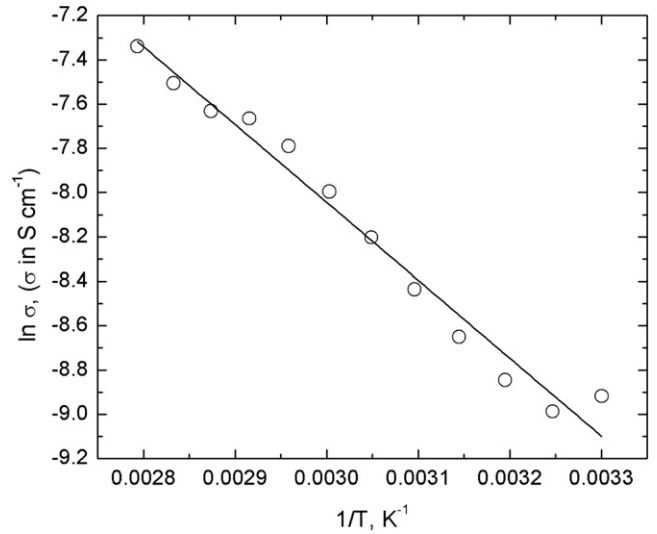


Fig. 14. Arrhenius plot showing the temperature dependence of the copolymer 8 membrane.

For an ideal membrane, $t_+ = 1$, and \bar{t}_+ is given by

$$\langle t_+^1 \rangle = E/E_{\max} \quad (3)$$

where E_{\max} is the electromotive force for an ideally permselective membrane obtained from Eq. (2) using $t_+^1 = 1$.

Values of the apparent proton and sodium ion transport numbers for different concentrations flanking the membrane are shown in Fig. 11. It can be seen that for very low concentrations the membrane is ideally permselective to protons and sodium ions, *i.e.* $\bar{t}_+ = 1$. This behavior is a consequence of the fact that co-ions are totally excluded from the membrane so that current is exclusively transported across the membrane by protons and sodium ions, respectively. As usual, the transport number decreases with increasing concentration of the electrolyte. At moderate and high concentrations, however, an increasing amount of coions intervene in the current transport across the membrane in such a way that the value of \bar{t}_+ comes close to that of \bar{t}_- . In this region, the transport number of Na^+ is slightly lower than that of H^+ .

The ohmic resistance of the membrane R_M in the acid form equilibrated with distilled water was measured at several temperatures. Two methods were used to determine the resistance of the membranes R_M , the Nyquist [26] and the Bode [27] diagrams. Illustrative Nyquist and Bode plots for the copolymer 8 membrane are shown in Figs. 12 and 13, respectively. The results obtained for R_M by the two methods are in rather good agreement. For example the value of R_M for the copolymer 8 membrane at 30 °C estimated from the former and the latter plots are respectively 20.24 Ω and 20.41 Ω .

Afterwards, the protonic conductivity was obtained by means of the familiar expression [28]

$$\sigma = \frac{l}{R_0 S} \quad (4)$$

where l and S are respectively thickness and area of the membrane in contact with the electrodes. The values of the proton conductivity obtained from the Nyquist and Bode diagrams is of $\sigma = 0.0135 \text{ S m}^{-1}$ and $\sigma = 0.0134 \text{ S m}^{-1}$ at 30 °C, respectively. The Arrhenius plot representing the temperature dependence of the

membrane, presented in Fig. 14, shows that the activation energy associated with proton transport across the copolymer **8** membrane is of 7.0 ± 0.4 kcal/mol. Taking into account the low ion-exchange capacity of the membranes, these results suggest that membranes with acceptable conductivity to be used as poly-electrolytes in low temperature fuel cells could be obtained by increasing the concentration of fixed $-\text{SO}_3^-$ groups in the chains.

4. Conclusions

A set of data concerning the copolymerization via ROMP of *N*-pentafluorophenyl-norbornene-5,6-dicarboximide (**1a**) and *N*-phenyl-norbornene-5,6-dicarboximide (**1b**) mixtures of *exo* (75%) and *endo* (25%) monomers at distinct molar ratios was processed by the Mayo-Lewis and Fineman-Ross methods to determine the copolymerization reactivity ratios. Using ruthenium alkylidene catalysts, random and block high molecular weight copolymers of **1a** with **1b** as well as **1a** with norbornene (**NB**) were synthesized, the main chains were hydrogenated and the perfluoroaromatic moieties were further sulfonated quantitatively to yield thermally enhanced, film forming ionomers which exhibited a high cationic permselectivity at low electrolyte concentrations. Permselectivity of the membranes to protons and sodium cations decreases with increasing the electrolyte concentration. The sulfonated copolymeric membranes absorb an unusual quantity of water despite their low IEC. It seems that microphases separation in the membranes serves to compartmentalize an excess of water into the polar side chain domains, specifically in the vicinity of the dicarboximide side groups.

Acknowledgements

Financial support from National Council for Science and Technology of Mexico (CONACYT) (PhD Scholarship to A.A.S.) is gratefully acknowledged. J. Vargas acknowledges CONACYT for a Posdoctoral Fellowship. We thank CONACYT-SEMARNAT and ICyTDF for generous support with contracts 23432 and 4312. We are grateful to Alejandrina Acosta, Salvador López Morales, Miguel Ángel Canseco and Carlos Flores Morales for their assistance in NMR, GPC, thermal properties and AFM, respectively. This work

was also supported by the CICYT through the project MAT2008-06725-C03-01.

References

- [1] Klok HA, Lecommandoux S. *Adv Mater* 2001;13:1217–29.
- [2] Bronich TK, Keifer PA, Shlyakhtenko LS, Kabanov AV. *J Am Chem Soc* 2005;127:8236–7.
- [3] Hagiopol C. *Copolymerization: toward a systematic approach*. New York: Kluwer Academic/Plenum; 1999.
- [4] Patton DL, Page KA, Xu C, Genson KL, Fasolka MJ, Beers KL. *Macromolecules* 2007;40(17):6017–20.
- [5] Tlenkopatchev MA, Vargas J, López-González MM, Riande E. *Macromolecules* 2003;36:8483–8.
- [6] Contreras AP, Tlenkopatchev MA, López-González MM, Riande E. *Macromolecules* 2002;35:4677–84.
- [7] Blackmore PM, Feast WJ. *J Fluorine Chem* 1988;40:331–47.
- [8] Dragutan V, Streck R. *Catalytic polymerization of cycloolefins*. Amsterdam: Elsevier; 2000.
- [9] Santiago AA, Vargas J, Gaviño R, Cerda AM, Tlenkopatchev MA. *Macromol Chem Phys* 2007;208:1085–92.
- [10] Tlenkopatchev M, Vargas J, Almaráz-Girón MA, López-González M, Riande E. *Macromolecules* 2005;38:2696–703.
- [11] Vargas J, Martínez A, Santiago AA, Tlenkopatchev MA, Gaviño R, Aguilar-Vega MJ. *Fluorine Chem* 2009;130:162–8.
- [12] Vargas J, Santiago AA, Tlenkopatchev MA, López-González M, Riande EJ. *Membr Sci* 2010;361:78–88.
- [13] Ghassemi H, McGrath JE, Zawodzinski Jr TA. *Polymer* 2006;47:4132–9.
- [14] Vargas J, Santiago AA, Tlenkopatchev MA, Gaviño R, Laguna MF, López-González M, et al. *Macromolecules* 2007;40:563–70.
- [15] Vargas J, Santiago AA, Tlenkopatchev MA, Gaviño R, Laguna MF, López-González MM, et al. *Adv Tech Mat Mat Proc J* 2007;9(2):135–40.
- [16] Berron BJ, Payne PA, Jennings GK. *Ind Eng Chem Res* 2008;47:7707–14.
- [17] Boyd TJ, Schrock RR. *Macromolecules* 1999;32(20):6608–18.
- [18] Santiago AA, Vargas J, Fomine S, Gaviño R, Tlenkopatchev MA. *J Polym Sci A Polym Chem* 2010;48:2925–33.
- [19] Mayo FR, Lewis FM. *J Am Chem Soc* 1944;66:1594–601.
- [20] Fineman M, Ross SD. *J Polym Sci* 1950;5:259–62.
- [21] Erbil C, Ozdemir S, Uyanik N. *Polymer* 2000;41:1391–4.
- [22] Szadkowska A, Makal A, Wozniak K, Kadyrov R, Grela K. *Organometallics* 2009;28:2693–700.
- [23] Vargas J, Santiago AA, Gaviño R, Cerda AM, Tlenkopatchev MA. *Express Polym Lett* 2007;1(5):274–82.
- [24] Badami AS, Lane O, Lee HS, Roy A, McGrath JE. *J Membr Sci* 2009;333:1–11.
- [25] Woodward AE. *Understanding polymer morphology*. New York: Hanser Publishers; 1995.
- [26] Nyquist H. *Phys Rev* 1928;32:110–3.
- [27] Bode WW. *Network analysis in feedback amplifier design*. Princeton, N. J.: Van Nostrand; 1956.
- [28] Sata T. *Ion exchange membranes*. Cambridge: The Royal Society of Chemistry; 2004 [Chapter 1].